Journal of Hydrology: Regional Studies 4 (2015) 661–674

Contents lists available at ScienceDirect

Journal of Hydrology: Regional Studies

journal homepage: www.elsevier.com/locate/ejrh

Development and evaluation of a physically-based lake level model for water resource management: A case study for Lake Buchanan, Texas

Peirong Lin [a], Zong-Liang Yang [a,*], Xitian Cai [a], Cédric H. David [b]

[a] Jackson School of Geosciences, University of Texas at Austin, Austin, TX, USA
[b] Jet Propulsion Laboratory, California Institute of Technology, Pasadena, CA, USA

ARTICLE INFO

Article history:
Received 6 December 2014
Received in revised form 15 August 2015
Accepted 19 August 2015
Available online 1 December 2015

Keywords:
Lake level and reservoir storage
Noah-MP
RAPID
Climate modeling
Decision-making

ABSTRACT

Study region: Lake Buchanan, a major reservoir for the City of Austin area, the Texas Hydrologic Region 12, USA.

Numerical climate models are increasingly being used by climate scientists to inform water management. However, successful transitions from climate models (O(10–100 km)) to water resources studies (O(100 m–1 km)) still need improved data structures and modeling strategies to resolve spatial scale mismatch. In this study, we introduce a mechanistic lake-level modeling framework that consists of a state-of-the-art land surface model – Noah-MP, a vector-based river routing scheme – RAPID, and a lake mass-balance model. By conducting a case study for Lake Buchanan, we demonstrate the capability of the framework in predicting lake levels at seasonal lead times. The experiments take into account different runoff resolutions, model initialization months, and multiple lead times. Uncertainty analyses and sensitivity tests are also conducted to guide future research.

New hydrological insights: Different from traditional grid-based solutions, the framework is directly coupled on the vector-based NHDPlus dataset, which defines accurate hydrologic features such as rivers, dams, lakes and reservoirs. The resulting hybrid framework therefore allows for more flexibility in resolving "scaling-issues" between large-scale climate models and fine-scale applications. The presented hindcast results also provide insight into the influences of baseline LSM resolutions, initialization months, and lead times, which would ultimately help improve lake-level forecast skills.

1. Introduction

Lakes and man-made reservoirs are important freshwater suppliers for domestic use, irrigation, livestock, and fishing (Sawunyama et al., 2006; Çimen and Kisi, 2009; Khatibi et al., 2014). Additionally, they are highly visible landscape features that affect aquatic ecosystems (Bednarek, 2001) and regional climates (Brekke et al., 2009). Seasonal outlooks of lake levels and reservoir storages could offer great socio-economic benefits as they determine "trigger points" (i.e., the designated points when specific actions are required) in real decision-making. If provided with reasonable accuracy, seasonal lake level predictions can guide and benefit water resources planning and management such as dam operations, water allocations,

* Corresponding author at: 2225 Speedway, Stop C1160, Austin, TX 78712-1692, USA. Fax: +1 512 471 9425.
E-mail address: liang@jsg.utexas.edu (Z.-L. Yang).

http://dx.doi.org/10.1016/j.ejrh.2015.08.005
2214-5818/

hydropower plans, and recreational activities. Consequently, development and evaluation of methodologies that better monitor and forecast lake-level variations continue to draw interest from both research community and operational agencies.

Currently, documented methodologies to model lake-level and reservoir storage variations can be categorized into three groups. The first group entails using statistical approaches to mimic fluctuating behaviors of lake inflows or direct lake levels based on historical time series. These approaches include, but not limited to multiple linear regression, stochastic modeling, autoregressive moving average, and artificial neural network (Faber and Stedinger, 2001; Khan and Coulibaly, 2006; Çimen and Kisi, 2009; Coulibaly, 2010; Khatibi et al., 2014) in various application settings. Second, space-based approaches take advantage of remote sensing and geographic information system (GIS) techniques (Sawunyama et al., 2006; Zhang et al., 2011; Gao et al., 2012) to derive relationships between remotely retrieved lake altimetry and surface area with lake levels and reservoir storages. These methodologies show great promise in providing monitoring capabilities especially for large lakes and reservoirs in data-sparse regions. The third group, which includes our framework, entails process-based approaches that utilize climate forecasts and physically-based, spatially-distributed hydrologic models (McGuire et al., 2006; Wilby, 2010), which is the focus of this study.

While each of these methodologies has advantages and limitations, we focus on developing and evaluating the climate and hydrologic model-based approaches due to the following considerations. First, these process-based approaches are mechanistic in nature, and hence do not require assumptions regarding hydrologic persistence or stationarity (Milly et al., 2008) that are utilized in statistical models. In addition, these modeling frameworks may facilitate follow-up studies on long-term projections of climatic impacts on water resources (e.g., Hamlet and Lettenmaier, 1999; Christensen et al., 2004; Yao et al., 2009; Haddeland et al., 2013) and seasonal forecasts of water supplies (e.g., Wood et al., 2002; Wood and Lettenmaier, 2006).

Despite several existing studies on process-based modeling frameworks, it is still challenging for water practitioners to use coarse-resolution gridded hydroclimate data for water resources studies (Kundzewicz and Stakhiv, 2010; Wilby, 2010) due to the lack of novel modeling strategies and data structures in combining large-scale models with fine-scale applications. To address this issue, Wood et al. (2011) proposed a "hyperresolution" modeling strategy and recommended the use of the high-resolution HydroSHEDS dataset (including vector-based river networks and drainage directions). Lehner and Grill (2013) used the HydroSHEDS dataset in their hydrologic model, and argued that the shift from grids to vectors would benefit "hyperresolution" modeling. Conceptually, the "object-oriented" organizations of data structures in a vectorized environment make the linkage among objects easier to handle than in a gridded environment. As more accurate GIS-based characterizations of hydrologic features become available, there is a growing need to consolidate them with grid-based climate and hydrologic models, and examine advantages and limitations of such hybrid frameworks. These GIS datasets include, but are not limited to lakes and reservoirs (Lehner and Döll, 2004), dams (Lehner et al., 2011), as well as river networks such as the HydroSHEDS (Lehner et al., 2006) and the National Hydrograph Dataset Plus (NHDPlus) (McKay et al., 2012).

The purpose of this study is thus to demonstrate an application of a hybrid modeling framework that supports both raster and vector data structures, and examine its applicability in predicting lake level changes. The Routing Application for Parallel computatIon of Discharge (RAPID) model is used because it simulates the river flows on the NHDPlus river network (vector- or reach-based) while being compatible with large-scale land surface models (LSMs). David et al. (2013) demonstrated that RAPID, coupled with four LSMs in the North American Data Assimilation System (NLDAS), is capable of well-simulating streamflow over the Texas Hydrologic Region 12. RAPID can also be coupled with catchment-based, rather than grid-based LSMs. In this study, the Noah LSM with multiple-parameterization options (Noah-MP) is used to provide runoff to feed RAPID. In the following sections, we first introduce the study area (Section 2), and then describe the modeling framework, implementation and datasets used (Section 3). Section 4 presents the results and conclusions. Finally, discussions on the modeling capabilities and limitations are provided.

2. Study area

The Texas Highland Lakes are a chain of seven man-made fresh water reservoirs located on the Colorado River Basin (CRB), the second largest basin in the Texas Hydrologic Region 12 (Region 12), draining an area of 102,172 km^2 to the Gulf of Mexico (Fig. 1). The six upper lakes, namely, Lake Buchanan, Inks Lake, Lake LBJ, Marble Falls, Lake Travis, and Lake Austin, were formed after dam constructions in the 1930s and 1940s. The Lower Colorado River Authority (LCRA) manages the six upper lakes to provide freshwater supply, flood control, irrigation, electricity, and recreational services around the City of Austin area, benefitting more than 1 million people. With a contributing area of 14,631 km^2, nearly 1/9 of the CRB, Lake Buchanan has the biggest surface area of around 90 km^2 and a maximum depth of around 40 m. Its storage capacity is around 1.08 km^3.

The Highland Lakes area features a semi-humid climate with annual rainfall ranging from 800 to 1000 mm. During the past 50 years, the region has experienced major droughts in 1950s, 1964, 1984, 2000, 2006, and 2011. As a result of low precipitation and high evaporation rates, the lake levels of Lake Buchanan have fallen below 301 meters above mean sea level, which is around 6 m below its long-term average. The extreme drought during 2011 has caused the lake level to drop dramatically, and even until late 2014 the reservoir remains less than 40% full, thereby largely impacting the agricultural uses and recreational activities of this region. The reservoir storage only recovered to ~70% full after successive rainfall during an anomalously wet season from March to May in 2015. Fig. 2(a) exhibits the long-term mean seasonal variations of

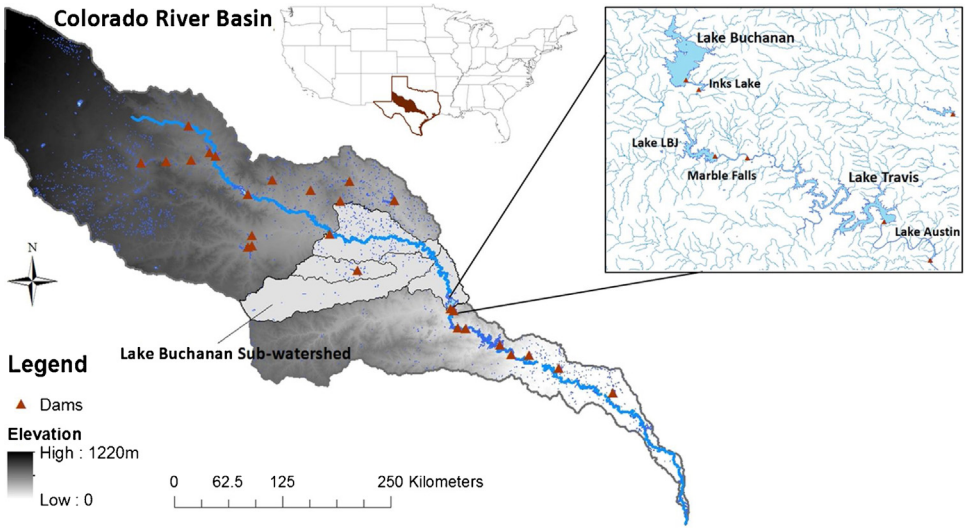

Fig. 1. Geographic location of Lake Buchanan and the six Highland Lakes in the lower Colorado River Basin, Texas, USA.

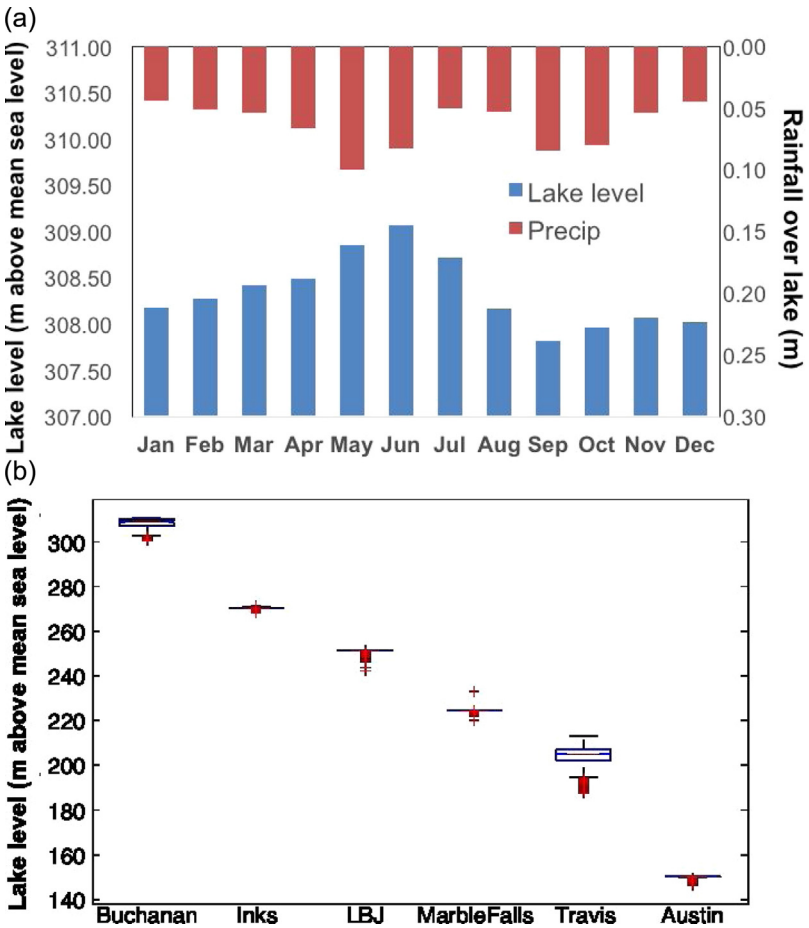

Fig. 2. (a) Seasonal variations of the Lake Buchanan water levels (long-term average using monthly data from 1979 to 2012); (b) Boxplot of the historical monthly mean lake levels of the six upper lakes.

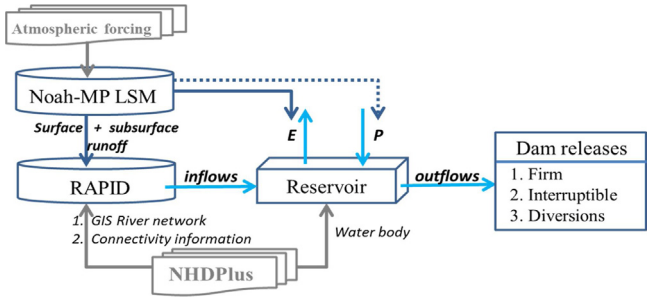

Fig. 3. Schematic diagram of the mechanistic modeling framework: four mass balance components are denoted in blue; supporting datasets are denoted in grey.

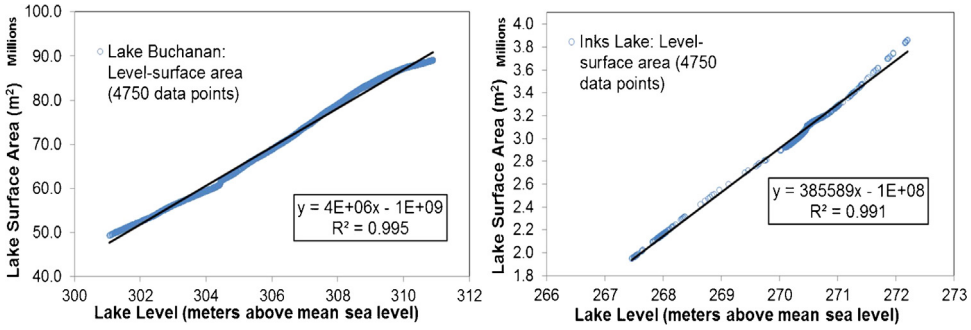

Fig. 4. Lake surface area–lake level relationships for Lake Buchanan and Inks Lake.

the Lake Buchanan levels (unit: meters above mean sea level). On average, the lake levels peak around May to June after a wet season in spring and then drop quickly during the ensuing dry hot summer; after another rainfall peak in the autumn, the lake levels slowly recover. The boxplot in Fig. 2(b) summarizes the historical lake level variations of the six upper lakes. Lake Buchanan and Lake Travis, two major reservoirs of the Highland Lakes, are more influenced by climatic conditions (e.g., precipitation and surface air temperature) while the other four are highly human-regulated (Fig. 3).

3. Data and model implementation

3.1. The modeling framework

In this study, lake-level changes are computed using the modeling framework shown in the schematic diagram above. The lake level–surface area relationship is predefined to convert the volumetric inflows and outflows to the correspondent lake-level changes in length. The groundwater–lake interaction is not explicitly considered because it is an elusive factor (Winter, 1981), which is beyond the scope of this study.

At each monthly time step t, the mass-balance model takes Eq. (1) to compute the lake level changes $\Delta L(t)$. Then hindcast is computed at the next time step $t+1$ based on Eq. (2):

$$\Delta L(t) = \frac{3600 \times 24 \times 30 \times [f_{\text{in}}(t) - f_{\text{out}}(t)]}{A(t-1)} + 0.001 \times [P(t) - E(t)] \quad (1)$$

$$L(t+1) = L(t) + \Delta L(t) \quad (2)$$

where the four mass-balance components are $f_{\text{in}}(t)$, the inflow rate from the main stream and tributaries as simulated by RAPID (in m^3/s); $f_{\text{out}}(t)$, the outflow rate (in m^3/s); $P(t)$, the direct precipitation the lake receives, and $E(t)$, the direct lake evaporation as calculated by Noah-MP (monthly total, in mm). $A(t)$ is the lake surface area (in m^2). The coefficients in Eq. (1) are used to uniform units. Through the linear fitting of historical data, a prior knowledge on the lake bathymetry is gained. Fig. 4 shows the lake surface area $A(t)$ as a function of lake level $L(t)$. Lake Buchanan has a more regular bathymetry than Inks Lake as the scattered dots are more evenly distributed across the full range. The derived relationship $A(t) = 4.403 \times 10^6 L(t) - 1.278 \times 10^9$ (coefficient of determination $R^2 = 0.995$) is used to update the Lake Buchanan surface area at each time step of the computation.

The experiments are driven by the 1-hourly North American Land Data Assimilation System Phase 2 (NLDAS-2) forcing, of which the precipitation field is a multi-source dataset that are topographically bias-adjusted for the continental U.S. (CONUS) at 0.125° spatial resolution (Cosgrove et al., 2003). Therefore NLDAS-2 is generally considered as an optimal input for hydrological applications

3.2. Model implementation

3.2.1. Reservoir inflows: the RAPID model

RAPID is a vector-based river routing model that uses a matrix-based Muskingum algorithm to solve the routing. It differs from traditional routing models in that it simulates the horizontal river transport on a reach-by-reach rather than grid-by-grid basis, and maintaining its compatibility with grid-based climate and hydrologic models. Essentially, RAPID takes the surface and subsurface runoff as calculated by LSMs or hydrologic models, and then based on the coupling algorithm as will be described in Eq. (3), it can "pour" the water generated on land surface grids into the vector channels of the NHDPlus (David et al., 2009, 2011, 2013a,b; Tavakoly et al., 2012) or the HydroSHEDS (David et al., 2015).

In this study, two runoff datasets that differ in spatial resolutions are used to feed the RAPID river flow simulations (RAPID v1.2.0, Zenodo, DOI:10.5281/zenodo.27242) and provide reservoir inflows with the aim of examining the lake level modeling sensitivity to the LSM resolutions—one is a Noah-MP 12.5-km runoff dataset simulated by this study, and the other is a Noah-MP 4.5-km runoff dataset as developed by David et al. (2013). Both experiments are driven by the same NLDAS-2 forcing but at different resolutions (i.e., original resolution at 12.5-km and interpolated forcing at 4.5-km resolution) and are completed from 2000 to 2007 for the entire Region 12. In total, two regional-scale streamflow simulations for the 68,143 river reaches in Texas are generated. Among them, 773 river reaches have direct USGS gauge stations, while 23,953 river reaches are headwater streams (i.e., 1st order streams according to the Strahler ordering system) that are almost all ungauged. Our analyses mainly focus on the streamflow simulations at the inlets of several major reservoirs in Texas for the purpose of reservoir water level modeling.

In the modeling framework, the "shift from grid to vector environment", which determines where river reaches get water from surrounding land surface grids, is achieved using the so-called "coupling algorithm" between LSM grids and vector river reaches with the aid of a set of catchment shapefiles provided by NHDPlus. More discussions about the coupling algorithm can be found in David et al., (2013). In this study, the coupling is achieved using the procedures described below. Each river reach i is associated with one local contributing catchment CC_i (area ranging from several to tens of square kilometers in our domain) in NHDPlus. The lateral inflow I_i that river reach i gets from surrounding LSMs grids is then determined by finding the runoff value where the centroid of CC_i lies, and the area of CC_i, which is A_{CCi}, I_i is therefore determined as:

$$I_i = (R_{s,i} + R_{b,i}) \times A_{CCi} \tag{3}$$

where $R_{s,i}$ and $R_{b,i}$ denote surface and subsurface runoff (baseflow), respectively. Because of the coupling algorithm formulation, the two RAPID simulations not only differ in their runoff generation processes, which are functions of the soil, vegetation, and land use parameters as defined by the underlying LSM resolutions; additionally, they differ in locations where the vector river reaches get water from LSM grid cells.

3.2.2. Lake evaporation and precipitation: the Noah-MP LSM

The community Noah LSM with multi-parameterization options (Noah-MP) was originally developed as the land surface component for the next-generation operational weather and climate forecasts. Its offline simulations have also been increasingly used to support various hydrological applications (e.g., Niu et al., 2011; Yang et al., 2011; Cai et al., 2014). Several hydrological enhancements were added to the multiple schemes of Noah-MP, such as an unconfined aquifer interacting with soil (Niu et al., 2007) and the landscape freeze/thaw properties (Shi et al., 2013), which improved the hydrological processes in the current LSMs. In this study, a simple TOPMODEL-based scheme in Noah-MP (Niu et al., 2005) is chosen for runoff parameterization, and the runoff is manually calibrated using three most sensitive factors as suggested by Cai et al. (2014) The model configured at 12.5-km resolution is used to estimate evaporation and precipitation over the lake area. In Noah-MP, Lake Buchanan is characterized as "water" according to the USGS land use land cover classification (value = 16), and the surrounding areas are "cropland/grassland mosaic" (value=5). The Penman-Monteith equation is solved to estimate evaporation over the water bodies, while precipitation is from the multi-source NLDAS-2 fields.

3.2.3. Reservoir outflows: a multiple linear regression scheme

A multiple linear regression scheme is used to estimate the reservoir outflow based on the inflow rate and water demand. Thus the outflow rate for month t can be written as:

$$f_{\mathrm{out},t} = a \times f_{\mathrm{in},t} + b \times D + c \tag{4}$$

where $f_{\mathrm{in},t}$ is the estimated reservoir inflow rate, D is the water demand, and a, b, c are three empirical coefficients. For multi-purpose reservoirs like Lake Buchanan, water demand in the actual water management consists of the amount used for hydropower generation, and the amount diverted or withdrawn to supply water for domestic, industrial and agricultural uses. While the former part is more positively correlated with inflow rates, the latter part is harder to characterize as it involves specific operating rules for different reservoirs and different climate scenarios such as droughts and floods. To simplify characterizations for water demand, the average percentage water demand for each month is empirically defined, accounting for the highest water demand in summer (JJA, assuming 60% of annual total water demand) due to the high needs for electricity and domestic uses, moderate water demand in spring and autumn (MAM and SON, each for 15%) due to agricultural uses, and low water demand in winter (DJF, 10%). Note that the seasonal variations of percentage water demand are derived by examining dam turbine release data (proxy for hydroelectricity demand) and dam diversion data (proxy for

Fig. 5. NHDPlus river network as RAPID model baselines: 14 inflows are marked in red.

domestic, industrial and agricultural demand). Assumptions are made that the demand is mainly season-dependent. Demand is therefore defined as 0.033, 0.033, 0.05, 0.05, 0.05, 0.2, 0.2, 0.2, 0.05, 0.05, 0.05, and 0.033 from January to December to represent the percentage water demand for each month. Multiple linear regression is then run based on Demand and the estimated monthly mean inflow rates (m^3/s) as calculated by R1 as it provides more accurate estimates of inflows, with a, b, c determined as 0.7831, 128.94, and −12.03, respectively. The coefficient of determination (R^2) is 0.65 for the regression, which is statistically significant ($p \ll 0.5$) for both inflow $f_{\text{in},t}$ and D. The derived equation is then used to model reservoir outflows based on inflows simulated by R1 and R2. In cases where the estimated outflow is predicted to be less than zero because of low inflow rates, outflow is determined as 50% of inflow (Wu and Chen, 2012) assuming half of the inflow will still be released in low flow period. This provides an estimated outflow for an active reservoir whose storage is beyond the dead storage. Based on this methodology, reservoir outflow is estimated during the lake level hindcast stage (Sections 4.1 and 4.2) and the results are compared with true historical release data (Section 4.1). The true dam release is obtained from LCRA from 2000 to 2007, which consists of gate release for flood control purposes, turbine release for hydropower generation, and the diversions for water supply.

4. Results and conclusions

4.1. Sources of uncertainties and modeling results

Fig. 5 shows the vectorized environment at the inlets of Lake Buchanan and a visual comparison between the NHDPlus and the HydroSHEDS river network. NHDPlus has higher accuracy and a better representation of hydrologic features than HydroSHEDS does. Digitalization of NHDPlus includes high-quality datasets such as aerial photography and paper maps provided by USGS NHD efforts (but only for the U.S.), while HydroSHEDS is a global-scale dataset derived from different resolution Shuttle Radar Topography Mission (SRTM) DEMs. NHDPlus keeps all headwater river reaches, while only river reaches that have a 25 km^2 upstream drainage area or more are retained in HydroSHEDS. Based on the NHDPlus river IDs (COMID in its attribute table), 14 connecting river reaches (marked in red) were selected to calculate the Lake Buchanan inflows.

Table 1 summarizes the RAPID performance in simulating reservoir inflows for Lake Buchanan and other major reservoirs in Texas. The performance is measured using R^2, Root Mean Square Error (RMSE, Eq. (4)), and normalized RMSE (NRMSE, Eq. (5)) to reflect timing errors, magnitude errors, and magnitude errors as referenced to mean annual streamflow. As large rivers tend to have larger RMSE than small streams, therefore mean annual streamflow values are used to normalize RMSE to provide a more objective assessments on the magnitude errors at different geographical locations. The two RAPID runs are denoted as R1 (coupled with 4.5-km gridded runoff) and R2 (coupled with 12.5-km gridded runoff), respectively.

$$\text{RMSE} = \sqrt{\frac{\Sigma_{i=1}^{n}\left(Q_{\text{obs},i} - Q_{\text{sim},i}\right)^2}{n}}$$

Table 1
Statistics of RAPID streamflow simulations upstream of several major reservoirs in Texas (eight years from 2000 to 2007, 96 months).

	Station name	Downstream reservoir	USGS gauge ID	RAPID river ID	Lat (N)	Lon (W)	R^2	RMSE (m^3/s)	NRMSE
1	Colr Rv Nr San Saba	Lake Buchanan	08147000	5756726	31°13′	98°33′	0.68(R1) 0.32(R2)	19.04(R1) 37.76(R2)	1.09(R1) 2.16(R2)
2	Llano Rv at Llano	Lake Buchanan	08151500	5771725	30°45′	98°40′	0.52(R1) 0.61(R2)	17.21(R1) 16.25(R2)	1.35(R1) 1.28(R2)
3	Buchanan Inflows	Lake Buchanan	\	14 inflow reaches	\	\	0.65(R1) 0.27(R2)	19.39(R1) 39.40(R2)	0.98(R1) 1.99(R2)
4	Neuces Rv nr Three Rivers	Corpus Christi Lake	08210000	3168766	28°25′	98°10′	0.66(R1) 0.68(R2)	43.65(R1) 70.80(R2)	1.57(R1) 2.54(R2)
5	Guadalupe Rv nr Spring Branch	Canyon Lake	08167500	3589120	29°51′	98°23′	0.88(R1) 0.86(R2)	12.19(R1) 18.50(R2)	0.63(R1) 0.96(R2)
6	Trinity Rv nr Crockett	Livingston Lake	08065350	1484774	31°20′	95°39′	0.91(R1) 0.67(R2)	58.24(R1) 124.25(R2)	0.34(R1) 0.73(R2)
7	Sabine Rv nr Beckville	Toledo Bend Reservoir	08022040	5278868	31°58′	94°00′	0.79(R1) 0.70(R2)	40.04(R1) 53.49(R2)	0.72(R1) 0.84(R2)
8	Chambers Ck nr Rice	Richland-Chambers Reservoir	08064100	1446962	32°11′	96°31′	0.46(R1) 0.36(R2)	13.84(R1) 15.11(R2)	1.29(R1) 1.41(R2)
9	Angelina Rv nr Alt	Sam Rayburn Reservoir	08036500	1150499	31°40′	94°57′	0.82(R1) 0.72(R2)	16.26(R1) 22.22(R2)	0.57(R1) 0.78(R2)

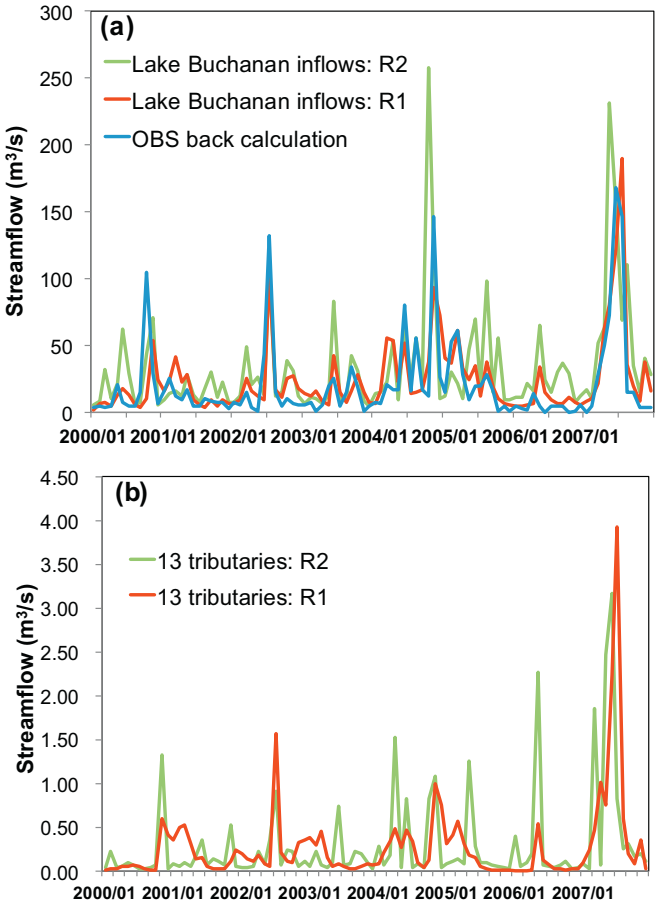

Fig. 6. (a) Hydrograph of Lake Buchanan inflows (one main stream and 13 headwater tributaries); (b) time series of tributary contributions.

$$\mathrm{NRMSE} = \mathrm{RMSE}/\overline{Q_{\mathrm{obs}}} \tag{5}$$

In general, RAPID simulations exhibit reasonably good skill scores for the USGS stations upstream of several major reservoirs. Specifically, the station above Lake Livingston (8.167.500) shows an R^2 skill score of ~0.9 for R1 and ~0.7 for R2, and the station above Canyon Lake (8.065.350) shows skills of ~0.9 for both R1 and R2. These two lakes play major roles in the water resource management for the city of Houston and the city of San Antonio, the fourth and seventh most populous cities in the U.S., respectively. The good simulation skills at the inlets of these major reservoirs in Texas show promise for expanding the applications to other regions. For two gauges right upstream of Lake Buchanan, the RAPID runs display skills of ~0.6. To evaluate the 14 direct Lake Buchanan inflows simulated by RAPID, we reversed the lake mass-balance model to infer the total inflows based on observed precipitation, evaporation, and actual dam releases (referred to as "OBS back calculation") as there are no direct gauge observations available at the lake inlets. Although the "observed" streamflow at the Lake Buchanan inlet is also subjected to errors due to uncertainties associated with the input data for the reversed mass-balance model, the estimate is considered as a reference to compare with model results. R1 shows a skill of 0.65 (higher than R2) in simulating direct lake inflows presumably because the land surface characterizations and the resulting parameters are better represented at finer LSM resolutions.

The hydrograph in Fig. 6a shows the river flow variations that contribute to Lake Buchanan are captured generally well by the RAPID simulations for the two types of runoff datasets, but R2 tends to over-estimate river flows during normal days. River flow simulations for the 13 headwater tributaries are also shown in Fig. 6b. It is noticed that the tributary contributions for Lake Buchanan are relatively small throughout the study time span, sometimes even smaller than the errors associated with the main stream simulations. However, the tributary contributions can be a large mass-balance component for certain regions that experience extreme flooding, in which case the present modeling framework could potentially add accuracy to the lake level modeling. However, the skills for the headwater tributary simulations still remain unclear due to limited gauge observations.

The reservoir outflows for R1 and R2 based on the multiple linear regression using the mean monthly percentage water demand and reservoir inflows are compared with the LCRA observed total dam releases (Fig. 7). The general release patterns

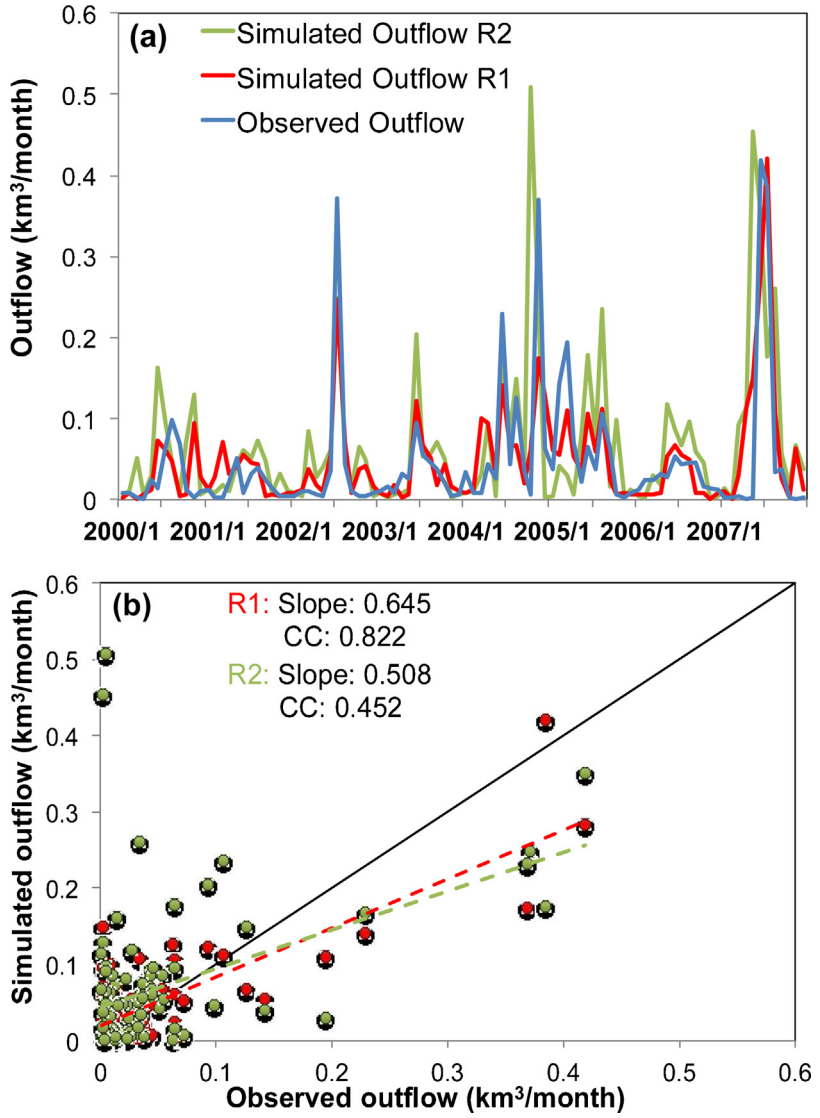

Fig. 7. (a) Time series comparison and (b) scatter plot between observed outflow and simulated outflow for R1 and R2 based on the multiple linear regression scheme.

are captured well by both simulations but R2 has a lower correlation coefficient (CC) because its inflows are subjected to more biases and timing problems. Both R1 and R2 capture the high outflows well, but the simulations for low outflows are more problematic as the high water demand, even during low flow days, is not sufficiently represented in the regression scheme.

The Noah-MP 12.5-km lake ET estimates are compared with two other observation-based data sources: (1) Texas Water Development Board (TWDB) lake evaporation estimate over 1° quadrangles (http://www.twdb.texas.gov/surfacewater/conditions/evaporation/), and (2) AVHRR remotely sensed 8-km ET product (Long et al., 2014). MODIS ET is generally considered as a better ET estimate from remote sensing techniques but since it does not address ET over water bodies, it is not used here. Compared with the two datasets, the Noah-MP lake ET estimate is biased high, with main differences lying in warm seasons when the total monthly ET is higher than 150 mm. This is consistent with Long et al.'s (2014) thorough comparison using a variety of LSM ET estimates and remotely sensed products. It is worth noting that the TWDB ET estimate originates from 76 pan evaporation stations, which has been carefully interpolated and multiplied by monthly pan-to-lake coefficients. However, the product is very likely to underestimate regional high ET values as it only stands for the 1° quadrangle averages. For the AVHRR ET, it uses the Penman-Monteith equation to estimate ET as Noah-MP does, but the driving surface meteorology is different. It uses the NCEP/NCAR reanalysis (Long et al., 2011), which was suggested as the worst-performing reanalysis for surface air temperature in a multi-reanalysis comparison study (Decker et al., 2012), while Noah-MP in this study was driven by a higher-resolution and higher-accuracy

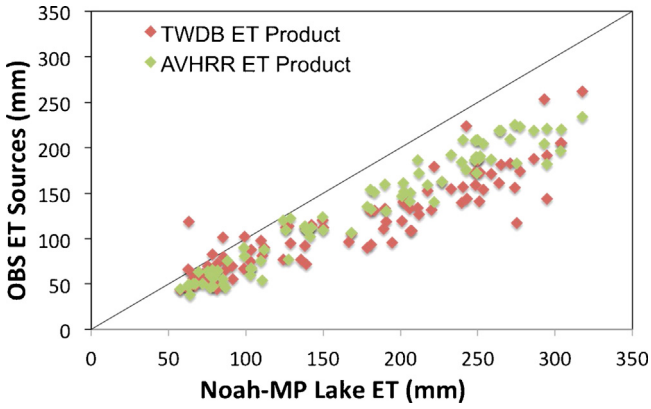

Fig. 8. Noah-MP lake ET estimate as compared with two other observational datasets.

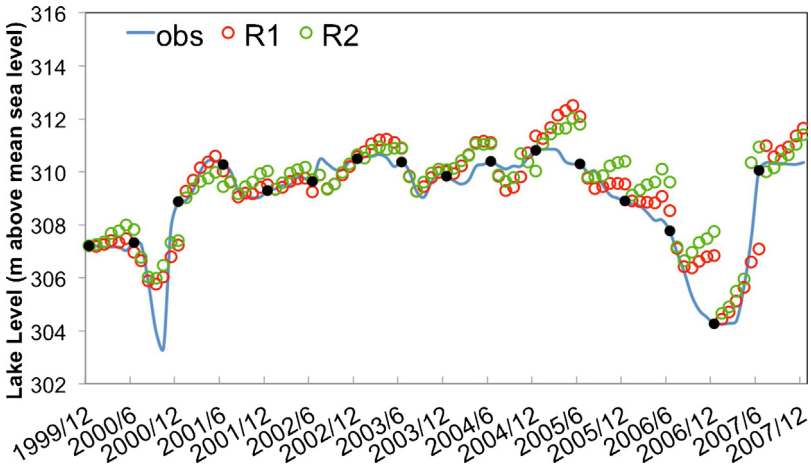

Fig. 9. Lake level predictions based on the proposed framework (black dots denote the time points when the mass-balance model is initialized).

NLDAS-2 forcing. Therefore, although the Noah-MP ET differs from the two observation datasets, it is still considered as a good estimate of ET for lake surfaces in the absence of better ET estimates such as from flux tower measurements for this region (Fig. 8).

Fig. 9 presents the time series of lake-level predictions assuming a six-month lead time. The computation starts with the observed lake level in December 1999, which is 307.21 meters above mean sea level; every six months, Eq. (2) is initiated using the observed lake levels obtained from gauged data. Within the six months interval, lake-level variations are predicted by the proposed modeling framework, which mainly reflects the cumulative errors in simulating the four mass balance components (more discussions in Section 4.3).

Generally, the lake levels are well reproduced, especially for years from 2001 to 2005 when the lake level variations are small. The lake level recoveries following two major droughts in 2000 and 2006 are very well-predicted by both simulations; by contrast, the water level drop caused by droughts is harder to capture. In another suite of lake-level prediction experiments using observed outflows (not shown), the water level drop in the 2000 drought is much better-captured than experiments using estimated outflow as shown here. This means the outflow under-estimation is mainly causing the problem in drought years. Both R1 and R2 have better performances in capturing the water level drop in 2000 than in 2006. Starting from 2005, the water level has several over-predictions. In particular, the over-prediction starting from December 2004 and December 2005 may be related to the under-predicted reservoir outflows, as the regression scheme for outflow estimation assumes low outflow rates during low inflow period as well as during winter to spring seasons, but the observed outflows suggest high values during these two periods. As for the over-prediction starting from June 2006, the outflow is well predicted but due to the over-prediction in inflow, the lake level is over-predicted. In general, R1 has better performances than R2 presumably because its inflow and outflow are better simulated than R2 (R2 tends to have an over-estimation of reservoir inflows). But there are situations when R2 out-performs R1 because the amount of outflows that is missing in the regression scheme can be cancelled out by the over-predicted outflows for R2. More discussions are provided below.

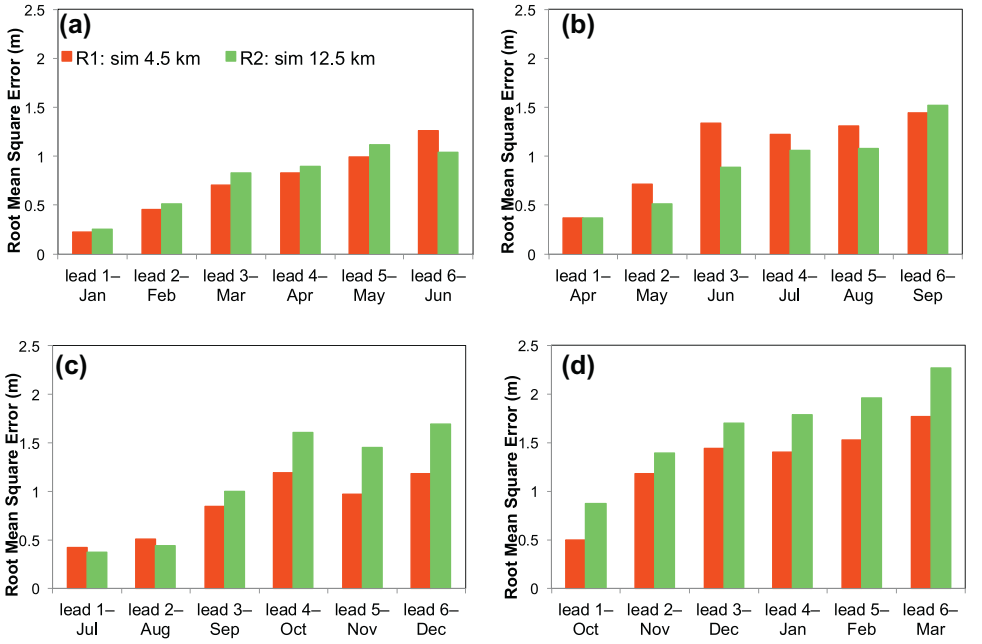

Fig. 10. Skill dependence of lake-level predictions at different lead times up to six months: model is initialized in (a) December (b) March (c) June (d) September of each year.

4.2. Skill dependence on multiple lead times

Fig. 10 shows the skill dependence of the lake-level predictions at multiple lead times and different initialization months. For all experiments *a*, *b*, *c* and *d*, the lake-level predictions are run to a maximum lead time of six months, but they are initialized in December, March, June, and September of each year, respectively.

Overall, the RMSEs of lake-level predictions grow with lead times. R2 is generally subject to more errors (ranging from 0.1 to 0.6 m) than R1 as R1 better estimates the inflow and the consequent outflow. However, R2 has a smaller RMSE than R1 during summer (JJA), which can be possibly ascribed to problems with the outflow regression scheme—during drought summers in JJA the actual dam releases are still high as determined by the river authority operations, but the regression scheme is under-predicting. Thus, the lake level is over-predicted. In this case, the over-estimated inflow in R2 would result in high outflow values that could compensate the missing amount of outflow from the regression scheme. It can be also concluded from Fig. 10 that for all lead times and for all initialization months, R1 has a mean RMSE of 0.99 m (on average 0.5 m RMSE for the first two lead months), indicating the effectiveness of R1 in lake-level predictions. For R2, the RMSEs are on average 0.1 m larger than that of R1. The hindcasts that are initiated in September are subjected to larger errors for both R1 and R2 (Fig. 10d), but those initiated in December, March and June have greater skills (Figs. 10a–c). In general, the reservoir inflow simulations are more sensitive to the LSM grid resolutions (reflected by differences between R1 and R2) than lake level predictions are, as the outflow errors may cancel out inflow errors in the computation based on mass balance. The Noah-MP/RAPID framework is able to provide a vectorized environment to compute lake level changes at fine scales, however, the skills are functions of initialization months, expected lead times, the LSM resolution and its coupling to the river reaches.

4.3. Sensitivity analysis

To better understand attribution of model uncertainties, we first present the four water budget components as contributions to lake level changes in length (m). The inflow in Fig. 11 is calculated using R1. The annual water budgets are averaged differentiating normal years and dry years of our study span.

For a freshwater reservoir like Lake Buchanan that has a surface area of around 90 km^2 and is under a semi-humid climate, the lake inflow and outflow are the two most influential factors driving the lake level variations, followed by evaporation loss over the lake area. The influence of evaporation becomes larger in dry years, taking up about 50–100% of the influences brought by inflows and outflows alone, but the inflow and outflow variations still dominate the water level changes. For this type of small- to medium-sized lakes, direct rainfall falling on the lake only takes up a small proportion of water level changes. On the other hand, rainfall that spreads over the large upstream contributing basin areas has a big influence on the lake inflows, causing lake level changes up to 1.8 m.

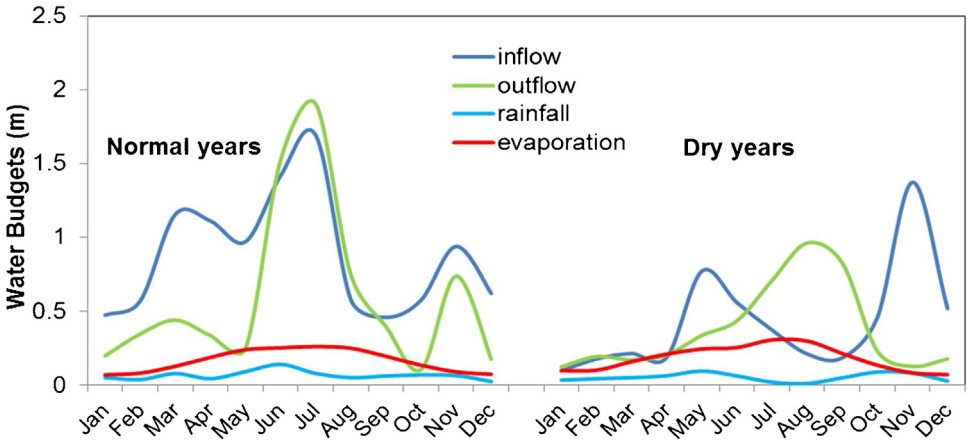

Fig. 11. Seasonal variations of four lake mass-balance components for Lake Buchanan: (left) normal year average from 2001 to 2005, and 2007; (right) dry year average in 2000 and 2006.

Table 2
Sensitivity analyses of the lake-level predictions (model is initialized each December and ran to a maximum of six-month lead).

Exp. No.	Input description	RMSE (m)					
		Lead 1–Jan	Lead 2–Feb	Lead 3–Mar	Lead 4–Apr	Lead 5–May	Lead 6–Jun
CTL	in, out, E, P by R1	0.23	0.46	0.71	0.83	0.99	1.26
Exp. 1	CTL, observed out	0.29	0.35	0.92	1.21	1.46	0.73
Exp. 2	CTL, mean monthly in	0.30	0.61	1.16	1.43	2.12	3.71
Exp. 3	CTL, mean monthly out	0.32	0.59	1.17	1.59	1.79	1.88
Exp. 4	CTL, mean monthly E	0.22	0.45	0.71	0.83	1.00	1.30
Exp. 5	CTL, mean monthly P	0.22	0.45	0.69	0.83	1.04	1.38

Below, we show some sensitivity analyses of the lake-level predictions by changing the lake model inputs. For simplicity, only R1 that is initialized in each December and at a maximum lead time of six months was conducted and evaluated in terms of RMSE. The control run (CTL) is the same as R1 in Experiment (a) (Fig. 10). Exp. 1 is the same as CTL except that the outflow is substituted by observed outflow values. For Exps. 2–5, the lake inflow (in), outflow (out), evaporation (E) and precipitation (P) are substituted by the 8-year averaged monthly in, out, E and P based on the best available data (i.e., R1 estimated inflow, LCRA outflow, TWDB ET and precipitation), respectively. In an actual lake level forecast case where the downscaled and bias-corrected atmospheric forcing in a forecast mode is used and certain assumptions on the lake outflows are made, it is very likely that only a rough seasonal variation (mean annual cycle) of these mass-balance components are captured. Therefore, it is helpful to estimate the prediction uncertainties one would expect to get if the predictions are only as good as the mean annual cycle of the in, out, E, and P. Table 2 summarizes the RMSEs for these tests. The RMSE increments between Exps. 2–5 and CTL reflect the error increases brought by the skill decreases of in, out, E, and P predictions, respectively.

As expected, the RMSE increments to CTL are largest to lowest for Exps. 2–5, which is consistent with Fig. 11 that predictions for inflow and outflow dominate the errors in lake level predictions, while the influences of predictions for E and P are small. If only a mean annual cycle of the four mass-balance component is captured in a real forecast, the overall influences are very limited within the first two lead months (nearly no RMSE increment in the first two columns). However for longer lead months, the errors start to accumulate and influence the lake level predictions. For Exp. 2 (monthly mean in), the RMSEs grow from 0.4 m to 2 m larger than CTL starting from the third to sixth lead months. For Exp. 3 (monthly mean out), the RMSEs only grow from 0.4 m to 0.7 m larger than CTL even for the longer lead months, which are more acceptable. For Exp. 4 and Exp. 5, ~0.1 m or less error is accumulated across all lead times, which means the influences of E and P are limited throughout. Additionally, for most lead times, Exp. 1 (using observed outflow) has larger RMSEs than CTL. This indicates that using estimated outflow helps reduce lake level prediction errors, as the errors in modeled inflow and outflow tend to cancel out. Overall, to get acceptable lake-level predictions at desired lead times, getting good predictions of the lake inflow and outflow is the top consideration. Our modeling framework shows consistently good predictions for both R1 and R2 up to 2- to 3-month lead times (within 0.5 m), but after 3-month lead times the reliability of using the framework depends largely on the prediction skills of reservoir inflows and outflows. For modeling Lake Buchanan water levels, a simulation of inflow (R^2 = 0.65) and outflow (R^2 = 0.67) could result in 0.22–1.26 m mean RMSE for lake level predictions up to 6-lead months starting from December. Future work is expected to improve the overall lake level predictions including the Noah-MP/RAPID model developments/calibrations and improved outflow estimation schemes.

5. Summary and discussions

This study focuses on development and evaluation of a mechanistic modeling framework to model lake-level changes, which innovatively combines a land surface model (Noah-MP), a large-scale river routing model (RAPID) and a lake mass-balance model. By conducting a case study in Lake Buchanan, a medium-sized reservoir that serves the hydroelectricity and freshwater supplies for the City of Austin, Texas, we show that the presented hybrid modeling framework, which supports both grid and vector data structures can facilitate fine-scale water management applications. The modeling capabilities and sources of uncertainties are also assessed based on the experimental runs over the historical period from 2000 to 2007.

The proposed modeling framework offers the following advantages. The overall package is capable of predicting the lake level variations of Lake Buchanan with reasonable accuracy. Noah-MP is a grid-based land surface model originally designed for global-scale weather and climate forecast studies, while the NHDPlus is a vector-based dataset that describes high-resolution and accurate hydrologic features (i.e., river network, connectivity, catchment, lakes, reservoirs, and dams) on the land surface of CONUS. Through the coupling of Noah-MP with RAPID on the NHDPlus dataset, the resulting package can simulate streamflow at regional to continental scales, meanwhile providing the reservoir inflows and other mass-balance component that are needed for lake-level modeling at fine scales. This framework can potentially serve as a useful tool for local water resource and lake management by providing a means to resolving aforementioned scaling issues.

The study is subject to the following limitations. (i) Only lumped parameter calibration is conducted for the entire Texas region. Further spatially-distributed parameter calibration would result in better accuracy in reservoir inflow simulations, and consequently better lake-level modeling. (ii) Model physics and the grid to vector coupling algorithm introduced in this study should be further improved towards the goal of decision-making processes. By examining two experiments that have different LSM spatial resolutions, we briefly mentioned that the RAPID streamflow simulations could be improved by finer representations of land surface characteristics, or possibly be degraded by the location shifts due to the grid to vector coupling process. It is suggested for Station 08151500 and 08210000 (see Table 1), the finer resolution run (R1) has an unexpected lower R^2 than the coarser-resolution run (R2). Further study is warranted to identify the skill dependence on LSM resolutions in the presented hybrid modeling framework and to improve the coupling algorithm. (iii) Groundwater-lake interactions are not considered in this study due to the simplified groundwater characterization in the current version of Noah-MP, and the poorly understood processes for groundwater-lake interactions at local scales. This component could potentially be large for certain regions, in which cases a more complicated groundwater model must be represented to more accurately model lake levels.

Acknowledgements

This work is supported by the NASA Interdisciplinary Science Program (award NNX11AJ43G), Microsoft Research and the Jackson School of Geosciences, University of Texas at Austin. Cédric H. David is supported by the Jet Propulsion Laboratory, California Institute of Technology, under a contract with NASA. The authors are grateful to Ronald Anderson (chief engineer in LCRA) for providing dam release data. Special thanks go to Dr. Di Long for helping with AVHRR data. Dr. Ahmad A. Tavakoly, Alex Resovsky, and Christopher Cacciatore are thanked for their help in enhancing quality of the manuscript.

Appendix A. Supplementary data

Supplementary data associated with this article can be found, in the online version, at http://dx.doi.org/10.1016/j.ejrh.2015.08.005.

References

Bednarek, A.T., 2001. Undamming rivers: a review of the ecological impacts of dam removal. Environ. Manage. 27, 803–814, http://dx.doi.org/10.1007/s002670010189.

Brekke, L.D., Maurer, E.P., Anderson, J.D., Dettinger, M.D., Townsley, E.S., Harrison, A., Pruitt, T., 2009. Assessing reservoir operations risk under climate change. Water Resour. Res., 45.

Cai, X., Yang, Z.-L., David, C.H., Niu, G.-Y., Rodell, M., 2014. Hydrological evaluation of the Noah-MP land surface model for the Mississippi River Basin. J. Geophys. Res. Atmos. 119, 23–38, http://dx.doi.org/10.1002/2013JD020792.

Christensen, N.S., Wood, A.W., Voisin, N., Lettenmaier, D.P., Palmer, R.N., 2004. The Effects of climate change on the hydrology and water resources of the Colorado river basin. Clim. Change 62, 337–363, http://dx.doi.org/10.1023/B:CLIM.13.684.13621.1f.

Çimen, M., Kisi, O., 2009. Comparison of two different data-driven techniques in modeling lake level fluctuations in Turkey. J. Hydrol. 378, 253–262, http://dx.doi.org/10.1016/j.jhydrol.2009.09.029.

Cosgrove, B.A., Lohmann, D., Mitchell, K.E., Houser, P.R., Wood, E.F., Schaake, J.C., Robock, A., Marshall, C., Sheffield, J., Duan, Q., Luo, L., Higgins, R.W., Pinker, R.T., Tarpley, J.D., Meng, J., 2003. Real-time and retrospective forcing in the North American Land Data Assimilation System (NLDAS) project. J. Geophys. Res. Atmos. 108, 8842, http://dx.doi.org/10.1029/2002JD003118.

Coulibaly, P., 2010. Reservoir computing approach to Great Lakes water level forecasting. J. Hydrol. 381, 76–88, http://dx.doi.org/10.1016/j.jhydrol.2009.11.027.

David, C.H., Gochis, D.J., Maidment, D.R., Yu, W., Yates, D.N., Yang, Z.-L., 2009. Using NHDPlus as the land base for the Noah-distributed Model. Trans. GIS 13, 363–377.

David, C.H., Maidment, D.R., Niu, G.-Y., Yang, Z.-L., Habets, F., Eijkhout, V., 2011. River network routing on the NHDPlus dataset. J. Hydrometeorol. 12, 913–934.

David, C.H., Yang, Z.-L., Hong, S., 2013a. Regional-scale river flow modeling using off-the-shelf runoff products, thousands of mapped rivers and hundreds of stream flow gauges. Environ. Model. Softw. 42, 116–132.

David, C.H., Yang, Z.-L., Famiglietti, J.S., 2013. Quantification of the upstream-to-downstream influence in the Muskingum method and implications for speedup in parallel computations of river flow. Water Resour. Res. 49, 2783–2800, http://dx.doi.org/10.1002/wrcr.20250.
David, C.H., Famiglietti, J.S., Yang, Z.-L., Eijkhout, V., 2015. Enhanced fixed-sized parallel speedup with the Muskingum method using a trans-boundary approach and a large sub-basins approximation. Water Resour. Res., http://dx.doi.org/10.1002/2014WR01665.
Decker, M., Brunke, M.A., Wang, Z., Sakaguchi, K., Zeng, X., Bosilovich, M.G., 2012. Evaluation of the reanalysis products from GSFC, NCEP, and ECMWF using flux tower observations. J Clim. 25, 1916–1944 http://dx.doi.org/10.1175/JCLI-D-11-00004.1.
Faber, B.A., Stedinger, J.R., 2001. SSDP reservoir models using ensemble streamflow prediction (ESP) forecasts. Am. Soc. Civil Eng., 1–10, http://dx.doi.org/10.1061/40569 (2001)00157.
Gao, H., Birkett, C., Lettenmaier, D.P., 2012. Global monitoring of large reservoir storage from satellite remote sensing. Water Resour. Res. 48, W09504, http://dx.doi.org/10.1029/2012WR012063.
Hamlet, A.F., Lettenmaier, D.P., 1999. Effects of climate change on hydrology and water resources in tHE Columbia river basin. JAWRA J. Am. Water Resour. Assoc. 35, 1597–1623.
Haddeland, I., Heinke, J., Biemans, H., Eisner, S., Flörke, M., Hanasaki, N., et al., 2013. Global water resources affected by human interventions and climate change. Proc. Natl. Acad. Sci. 111 (9), 3251–3256.
Khan, M., Coulibaly, P., 2006. Application of support vector machine in lake water level prediction. J. Hydrol. Eng. 11, 199–205, http://dx.doi.org/10.1061/(ASCE) 1084-0699(2006)11:3(199).
Khatibi, R., Ghorbani, M.A., Naghipour, L., Jothiprakash, V., Fathima, T.A., Fazelifard, M.H., 2014. Inter-comparison of time series models of lake levels predicted by several modeling strategies. J. Hydrol. 511, 530–545, http://dx.doi.org/10.1016/j.jhydrol.2014.01.009.
Kundzewicz, Z.W., Stakhiv, E.Z., 2010. Are climate models ready for prime time in water resources management applications, or is more research needed? Hydrol. Sci. J. 55, 1085–1089, http://dx.doi.org/10.1080/02626667.2010.513211.
Lehner, B., Döll, P., 2004. Development and validation of a global database of lakes, reservoirs and wetlands. J. Hydrol. 296, 1–22.
Lehner, B., Verdin, K., Jarvis, A., 2006. HydroSHEDS Technical Documentation, Version 1.0. World Wildlife Fund US, Washington, DC, pp. 1–27.
Lehner, B., Grill, G., 2013. Global river hydrography and network routing: baseline data and new approaches to study the world's large river systems. Hydrol. Process. 27, 2171–2186, http://dx.doi.org/10.1002/hyp.9740.
Lehner, B., Liermann, C.R., Revenga, C., Vörösmarty, C., Fekete, B., Crouzet, P., Döll, P., Endejan, M., Frenken, K., Magome, J., Nilsson, C., Robertson, J.C., Rödel, R., Sindorf, N., Wisser, D., 2011. High-resolution mapping of the worldös reservoirs and dams for sustainable river-flow management. Front. Ecol. Environ. 9, 494–502, http://dx.doi.org/10.1890/100125.
Long, D., Longuevergne, L., Scanlon, B.R., 2014. Uncertainty in evapotranspiration from land surface modeling, remote sensing, and GRACE satellites. Water Resour. Res. 50, 1131–1151, http://dx.doi.org/10.1002/2013WR014581.
McGuire, M., Wood, A., Hamlet, A., Lettenmaier, D., 2006. Use of satellite data for streamflow and reservoir storage forecasts in the Snake river basin. J. Water Resour. Plan. Manage. 132, 97–110, http://dx.doi.org/10.1061/(ASCE) 0733-9496(2006)132:2(97).
McKay, L., Bondelid, T., Rea, A., Johnston, C., Moore, R., Deward, T., 2012. NHDPlus Version 2: user guide: 168.
Milly, P.C.D., Betancourt, J., Falkenmark, M., Hirsch, R.M., Kundzewicz, Z.W., Lettenmaier, D.P., Stouffer, R.J., 2008. Stationarity is dead: whither water management? Science 319, 573–574, http://dx.doi.org/10.1126/science.1151915.
Niu, G.-Y., Yang, Z.-L., Dickinson, R.E., Gulden, L.E., 2005. A simple TOPMODEL-based runoff parameterization (SIMTOP) for use in global climate models. J. Geophys. Res. Atmos. 1984–2012, 110.
Niu, G.-Y., Yang, Z.-L., Dickinson, R.E., Gulden, L.E., Su, H., 2007. Development of a simple groundwater model for use in climate models and evaluation with gravity recovery and climate experiment data. J. Geophys. Res. 112, D07103, http://dx.doi.org/10.1029/2006JD007522.
Niu, G.-Y., Yang, Z.-L., Mitchell, K.E., Chen, F., Ek, M.B., Barlage, M., Kumar, A., Manning, K., Niyogi, D., Rosero, E., 2011. The community Noah land surface model with multiparameterization options (Noah-MP): 1. Model description and evaluation with local-scale measurements. J. Geophys. Res. Atmos. 1984–2012, 116.
Shi, M., Yang, Z.-L., Landerer, F.W., 2013. Representing and evaluating the landscape freeze/thaw properties and their impacts on soil impermeability: Hydrological processes in the community land model version 4. J. Geophys. Res. Atmos. 118, 7542–7557, http://dx.doi.org/10.1002/jgrd.50576.
Tavakoly, A.A., David, C.H., Maidment, D.R., Yang, Z.-L., 2012. An upscaling process for large-scale vector-based river networks using the NHDPlus dataset. In: Proceedings of the American Water Resources Association Spring Specialty Conference on Geographic Information Systems and Water Resources, March, 2012.
Sawunyama, T., Senzanje, A., Mhizha, A., 2006. Estimation of small reservoir storage capacities in Limpopo River Basin using geographical information systems (GIS) and remotely sensed surface areas: case of Mzingwane catchment. Phys. Chem. Earth Parts ABC, 935–943, http://dx.doi.org/10.1016/j.pce.2006.08.008.
Wilby, R.L., 2010. Evaluating climate model outputs for hydrological applications. Hydrol. Sci. J. 55, 1090–1093, http://dx.doi.org/10.1080/02626667.2010.513212.
Winter, T.C., 1981. Uncertainties in estimating the water balance of lakes. JAWRA J. Am. Water Resour Assoc. 17, 82–115, http://dx.doi.org/10.1111/j.1752-1688.1981.tb02593.x.
Wood, A.W., Lettenmaier, D.P., 2006. A test bed for new seasonal hydrologic forecasting approaches in the Western United States. Bull. Am. Meteorol. Soc. 87, 1699–1712, http://dx.doi.org/10.1175/BAMS-87-12-1699.
Wood, A.W., Maurer, E.P., Kumar, A., Lettenmaier, D.P., 2002. Long-range experimental hydrologic forecasting for the eastern United States. J. Geophys. Res. Atmos. 1984–2012 107, ACL–6.
Wood, E.F., et al., 2011. Hyperresolution global land surface modeling: meeting a grand challenge for monitoring Earth's terrestrial water. Water Resour Res. 47, W05301, http://dx.doi.org/10.1029/2010WR010090.
Wu, Y., Chen, J., 2012. An operation-based scheme for a multiyear and multipurpose reservoir to enhance macroscale hydrologic models. J. Hydrometeor. 13, 270–283 http://dx.doi.org/10.1175/JHM-D-10-05028.1.
Yang, Z.-L., Niu, G.-Y., Mitchell, K.E., Chen, F., Ek, M.B., Barlage, M., Longuevergne, L., Manning, K., Niyogi, D., Tewari, M., 2011. The community Noah land surface model with multiparameterization options (Noah-MP): 2. Evaluation over global river basins. J. Geophys. Res. Atmos. 1984–2012, 116.
Yao, H., Scott, L., Guay, C., Dillon, P., 2009. Hydrological impacts of climate change predicted for an inland lake catchment in Ontario by using monthly water balance analyses. Hydrol. Process. 23, 2368–2382, http://dx.doi.org/10.1002/hyp.7347.
Zhang, G., Xie, H., Kang, S., Yi, D., Ackley, S.F., 2011. Monitoring lake level changes on the Tibetan Plateau using ICESat altimetry data (2003–2009). Remote Sens. Environ. 115 (7), 1733–1742, ISSN 0034-4257.